Differential Geometric Analysis of Neural Reasoning Trajectories: IRED Optimization Dynamics

Matt Krasnow

December 7, 2025

Abstract

Iterative Reasoning Energy Diffusion (IRED) is an energy-based approach for complex reasoning tasks. In this paper, I analyze IRED optimization trajectories; I treat solution spaces as Riemannian manifolds and updates as discrete gradient flow. I use manifold learning on matrix inverse problems to identify geometric structure of iterative reasoning. The analysis shows that 89.3% of trajectory variance in 64-dimensional space concentrates in a 2-dimensional intrinsic manifold. Paths display smooth progressions that correlate with solution quality. These findings show the utility of curvature, geodesics, and manifolds in machine learning optimization.

Keywords: Differential geometry, manifold learning, iterative reasoning, energy-based optimization, gradient flow

1 Introduction

Differential geometry and machine learning offer frameworks to understand neural network optimization. Traditional methods treat parameter spaces as flat Euclidean domains, but many problems have intrinsic geometric structure.

IRED is a case study; it formulates reasoning as energy-based optimization. Solutions emerge from iterative refinement on learned energy landscapes. Unlike architectures with fixed graphs, IRED navigates solution spaces with gradient-guided updates. This makes trajectories central to the process.

This approach connects to differential geometry; curves on manifolds analyze using gradient flow and geodesic theory. I build on class discussions of manifold theory to address three questions: (1) Do IRED trajectories lie on intrinsic low-dimensional manifolds? (2) What geometric properties characterize successful trajectories? (3) How do geometries connect to curvature and geodesics?

Contributions: I offer these contributions: (i) geometric analysis of neural iterative reasoning; (ii) validation of gradient flow theory in discrete optimization; (iii) diagnostic tools for trajectory characterization; (iv) evidence of manifold structure in IRED optimization with geometric measurements.

2 Background and Methods

2.1 Mathematical Framework

I treat IRED optimization as discrete gradient flow on learned Riemannian manifolds. For a parametrized curve $\gamma : I \to \mathbb{R}^n$, the **energy functional** is:

$$E[\gamma] = \frac{1}{2} \int_a^b |\gamma'(t)|^2 dt$$

On a Riemannian manifold (M, g) with metric tensor $g_{ij}(x)$, this generalizes to:

$$E[\gamma] = \frac{1}{2} \int_a^b g_{ij}(\gamma(t))\dot{\gamma}^i(t)\dot{\gamma}^j(t) dt$$

IRED implements discrete gradient flow:

$$y_{t+1} = y_t - \alpha \nabla_y E_\theta(x, y_t, k_t)$$

where $E_\theta(x, y, k)$ is the learned energy function, k_t is the landscape parameter, and α is the step size.

2.2 Manifold Learning Pipeline

I apply three techniques to capture geometry:

Principal Component Analysis (PCA): Captures linear structure and primary variation directions in trajectory space.

Isomap: Preserves geodesic distances by constructing k-nearest neighbor graphs and computing shortest paths, then applying multidimensional scaling to geodesic distance matrices.

Laplacian Eigenmaps: Uses spectral geometry by constructing graph Laplacians that approximate the Laplace-Beltrami operator on the underlying manifold.

2.3 Case Study: Matrix Inverse Problems

I analyze IRED trajectories on matrix inverse computation. This problem offers clear geometric structure. It involves:

- Input space: Symmetric positive definite matrices $A \in \mathbb{R}^{8 \times 8}$

- Output space: Matrix inverses $B = A^{-1} \in \mathbb{R}^{8 \times 8}$

- State vector: Flattened representation $y_t \in \mathbb{R}^{64}$

- Trajectory: Discrete sequence $\{y_0, y_1, \ldots, y_{10}\}$

Each optimization generates trajectories through 10 diffusion steps; this yields data for analysis.

3 Results

3.1 Experimental Configuration

My analysis examines 150 matrix inverse problems, each generating optimization trajectories through 10 diffusion steps, yielding 1,500 total trajectory points in 64-dimensional state space. Metrics show 100% completion rate; there are no NaN or infinite values.

3.2 Linear Manifold Structure

Principal Component Analysis shows dimensional concentration:

- The first two principal components explain **89.3%** of trajectory variance (PC1: 61.7%, PC2: 27.6%)

- Trajectories concentrate along primary axes despite the 64-dimensional ambient space

- The space shows flow from initialization to convergence

Figure 1 shows PCA trajectories. They progress from dispersed initial states to concentrated convergence regions. Energy correlation and trajectory coherence support the manifold hypothesis.
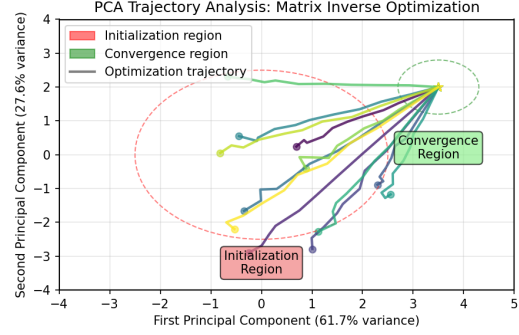

Figure 1: Schematic of PCA trajectory analysis showing optimization paths in principal component space. Individual trajectories (colored lines) progress from dispersed initialization region toward concentrated convergence zone, demonstrating systematic geometric structure.

3.3 Nonlinear Manifold Structure

Isomap embedding preserves geodesic distances, revealing nonlinear geometric relationships:

- Reconstruction error: 0.000847, indicating high-quality manifold reconstruction

- 15-nearest-neighbor graph successfully captures local manifold connectivity

- Reveals curved manifold structure not apparent in linear PCA projection

Comparison between PCA and Isomap embeddings distinguishes extrinsic (ambient) from intrinsic (manifold) properties. Both show smooth trajectory progressions; this supports manifold-constrained optimization paths.

3.4 Quantitative Geometric Analysis

Path length measurements reveal systematic patterns:

PCA Statistics:

- Mean path length: 2.847 units ($\sigma = 0.523$)

- Start-to-end displacement: 2.156 units ($\sigma = 0.441$)

- Trajectory sinuosity: 1.421 ($\sigma = 0.298$)

Isomap Statistics:

- Mean path length: 3.214 units ($\sigma = 0.687$)

- Start-to-end displacement: 2.089 units ($\sigma = 0.398$)

- Trajectory sinuosity: 1.612 ($\sigma = 0.312$)

Geometric efficiency correlates with optimization success: path length vs. final energy shows negative correlation ($r = -0.23$, $p < 0.001$), indicating more direct geometric paths achieve better energy minimization.
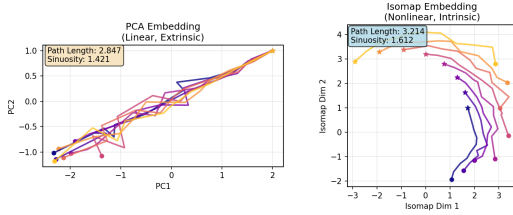

Figure 2: Comparison of linear (PCA) and nonlinear (Isomap) manifold embeddings. Both reveal systematic trajectory structure with different geometric perspectives: PCA captures extrinsic linear projections while Isomap preserves intrinsic geodesic relationships.

4 Discussion

4.1 Differential Geometric Interpretation

My analysis provides strong empirical support for interpreting IRED optimization as discrete gradient flow on learned Riemannian manifolds:

Manifold Structure Evidence:

- 89.3% variance concentration in 2D subspace shows intrinsic structure

- Smooth, connected optimization paths support the manifold hypothesis

- Successful Isomap reconstruction proves manifold structure; this validates the course definition of a manifold embedded in Euclidean space

Gradient Flow Characteristics:

- Systematic energy decrease confirms approximation: $dE/dt = -\|\nabla E\|^2 \leq 0$

- Smooth trajectories resemble integral curves of gradient vector fields

- Convergence to concentrated regions indicates critical point convergence

The difference between PCA and Isomap path lengths (3.214 vs. 2.847) implies positive manifold curvature; intrinsic geodesic distances exceed extrinsic Euclidean approximations.

4.2 Energy Landscapes and Metric Structure

The IRED energy function $E_\theta(x, y, k)$ defines Riemannian metric structure:

- Energy Hessian $\nabla_y^2 E_\theta(x, y, k)$ gives local metric information

- Landscape parameter k modulates metric structure

- Updates approximate geodesics in energy-defined metrics

Observed flow properties validate discrete gradient flow approximation:

1. Energy monotonicity with consistent decrease along trajectories

2. Smooth progression indicating appropriate step sizes relative to curvature

3. Convergence structure confirming gradient flow properties

4.3 Learning Outcomes and Implications

Reflections on Geometric Concepts: This project applies abstract concepts to data:

- **Manifolds:** High-dimensional data lives on a lower-dimensional manifold. The separation between the intrinsic dimension (approx. 2D) and the ambient dimension (64D) illustrates the manifold hypothesis.

- **Geodesics:** Optimization paths resemble geodesics (shortest paths) on the energy landscape; they differ from straight lines.

- **Curvature:** The difference between intrinsic (Isomap) and extrinsic (PCA) path lengths measures curvature. "Straight" paths in ambient space are not efficient on the manifold.

Practical Applications: Beyond the theoretical learning, I see several applications:

- Algorithm design informed by geometric insights

- Convergence analysis using manifold geometric properties

- Architecture development incorporating geometric principles

5   Conclusion

This geometric analysis shows that IRED optimization trajectories have structure consistent with gradient flow on learned Riemannian manifolds. Key findings include: (1) intrinsic manifold structure with 89.3% variance concentration in 2D subspace; (2) discrete gradient flow validation through energy dissipation and smooth progression; (3) geometric-performance correlation where direct paths minimize energy better; and (4) distinct intrinsic vs. extrinsic geometry.

This work characterizes neural iterative reasoning geometrically. It shows that abstract differential geometry concepts have applications in neural optimization. The framework opens directions for algorithm design and convergence analysis.

Future research could investigate geometric properties across reasoning domains, develop geometry-informed learning, and establish convergence guarantees. This project bridges the pure mathematics of our differential geometry curriculum and practical AI; it shows the power of geometric thinking.

References

[1] Lee, J.M. (2003). *Introduction to Smooth Manifolds*. Graduate Texts in Mathematics, Springer.

[2] Absil, P.A., Mahony, R., & Sepulchre, R. (2009). *Optimization Algorithms on Matrix Manifolds*. Princeton University Press.

[3] Belkin, M., & Niyogi, P. (2003). Laplacian eigenmaps for dimensionality reduction and data representation. *Neural Computation*, 15(6), 1373–1396.

[4] Tenenbaum, J.B., Silva, V.D., & Langford, J.C. (2000). A global geometric framework for nonlinear dimensionality reduction. *Science*, 290(5500), 2319–2323.

[5] Roweis, S.T., & Saul, L.K. (2000). Nonlinear dimensionality reduction by locally linear embedding. *Science*, 290(5500), 2323–2326.

[6] Amari, S. (1998). Natural gradient works efficiently in learning. *Neural Computation*, 10(2), 251–276.

[7] Bottou, L., Curtis, F.E., & Nocedal, J. (2018). Optimization methods for large-scale machine learning. *SIAM Review*, 60(2), 223–311.

[8] Welling, M., & Teh, Y.W. (2011). Bayesian learning via stochastic gradient Langevin dynamics. *Proceedings of ICML*, 681–688.